

# Accepted Manuscript

Efficient removal of oil from oil contaminated water by superhydrophilic and underwater superoleophobic nano/micro structured TiO<sub>2</sub> nanofibers coated mesh

Udara Bimendra Gunatilake, Jayasundera Bandara

PII: S0045-6535(16)31743-X

DOI: [10.1016/j.chemosphere.2016.12.031](https://doi.org/10.1016/j.chemosphere.2016.12.031)

Reference: CHEM 18486

To appear in: *ECSN*

Received Date: 30 July 2016

Revised Date: 3 December 2016

Accepted Date: 7 December 2016

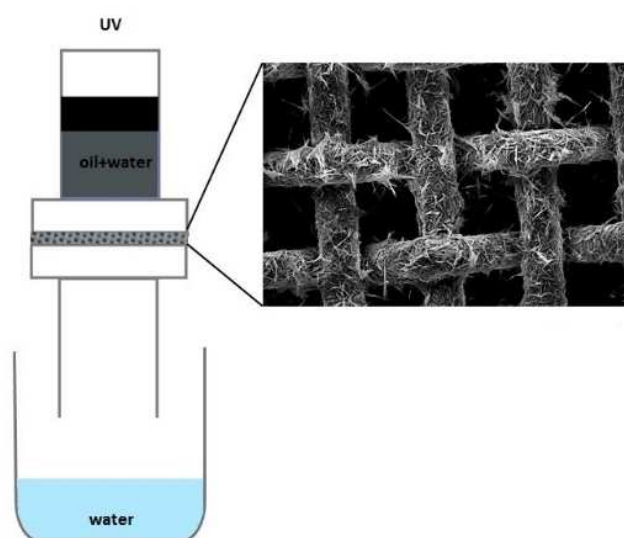
Please cite this article as: Gunatilake, U.B., Bandara, J., Efficient removal of oil from oil contaminated water by superhydrophilic and underwater superoleophobic nano/micro structured TiO<sub>2</sub> nanofibers coated mesh, *Chemosphere* (2017), doi: 10.1016/j.chemosphere.2016.12.031.

This is a PDF file of an unedited manuscript that has been accepted for publication. As a service to our customers we are providing this early version of the manuscript. The manuscript will undergo copyediting, typesetting, and review of the resulting proof before it is published in its final form. Please note that during the production process errors may be discovered which could affect the content, and all legal disclaimers that apply to the journal pertain.



**Graphical abstract**

The TiO<sub>2</sub> nanofibers coated stainless steel mesh as a novel underwater superoleophobic membrane for the effective separation of contaminated oil-water mixtures is reported.



1 **Efficient removal of oil from oil contaminated water by**  
2 **superhydrophilic and underwater superoleophobic nano/micro**  
3 **structured TiO<sub>2</sub> nanofibers coated mesh**

4 Udara Bimendra Gunatilake and Jayasundera Bandara\*

5 National Institute of Fundamental Studies, Hantana Road, CP 20000, Kandy, Sri Lanka

6 Email: Jayasundera Bandara: bandaraj@ifs.ac.lk; jayasundera@yahoo.com, Tel:+94 812232002

7 **ABSTRACT**

8 In this report, we investigated the TiO<sub>2</sub> nanofibers coated stainless steel mesh as a novel  
9 underwater superoleophobic membrane for the effective separation of contaminated oil-water  
10 mixtures. The membrane was fabricated by spray deposition of hydrothermally synthesized TiO<sub>2</sub>  
11 nanofibers on stainless steel mesh. The fabricated membrane exhibits superhydrophilicity and  
12 superoleophobicity properties in air and underwater respectively allowing the separation of oil-  
13 water efficiently. Randomly deposited TiO<sub>2</sub> nanofibers on mesh exhibit rough surface property  
14 and hence superhydrophilic nature. Water oil separation efficiencies of ~90 and ~99% were  
15 achieved with this filter for less viscous and highly viscous oil respectively. Additionally, the  
16 TiO<sub>2</sub> nanofibers coated mesh can degrade immiscible organic molecules due to photocatalytic  
17 activity of TiO<sub>2</sub> nanofibers under UV light. As a result of self-cleaning property of TiO<sub>2</sub>  
18 nanofibers coated mesh, the durability of the filter membrane was enhanced.

19 **KEYWORDS:** TiO<sub>2</sub> nanofibers, underwater superoleophobicity, oil-water separation,  
20 superhydrophilic, photocatalytic activity, super-wetting membrane

## 21 INTRODUCTION

22 Water pollution through immiscible and miscible oil is a major problem that each and  
23 every industrially revolutionized country has to face. Discharge of the oil polluted water to the  
24 environment without purification or pretreatment is a major threat to the human beings and to the  
25 whole ecosystem (Fosberg, 1974; Odeigah et al., 1997; Liu and Diamond, 2005; Olsson, 2015).  
26 Scientists anticipate new advanced techniques to clean up oil spills from water exceeding the  
27 traditional oil wastewater treatment methods such as coagulation and flocculation techniques  
28 (Bratby, 1980; Al-Shamrani et al., 2002; Inan et al., 2004), advanced chemical oxidation  
29 techniques (Munter, 2001; Schrank et al., 2004; Bautista et al., 2008; Xu et al., 2012), adsorption  
30 techniques (Balba et al., 1998; Mitchell et al., 2002; Gaya and Abdullah, 2008; Gur-Reznik et al.,  
31 2008; Fakhru'l-Razi et al., 2009; Pyrzynska, 2011), electrochemical/photocatalytic treatment  
32 methods (Ma and Wang, 2006; Chong et al., 2010) and biological treatment methods (Rosal et  
33 al., 2010; Xia et al., 2010).

34 On the other hand, currently, enormous demands do exist on the special wetting materials  
35 to fabricate oil water separating filter membranes due to their efficiency and the cost  
36 effectiveness (Yao et al., 2011; Xue et al., 2014; Dunderdale et al., 2015). These membranes can  
37 be integrated to the existing physical reactors of cleaning processes of the oil/water separating  
38 plants. In this respect, materials with superhydrophobic and superoleophilic properties have  
39 been intensively investigated in applying wastewater purification in last few decades (Wang et  
40 al., 2006; Lee et al., 2011; Xu et al., 2016). The major disadvantage of these gravity driven filter  
41 membranes with superhydrophobic and superoleophilic materials is that they easily get blocked  
42 and fouled by viscous/dense oil and affecting the oil-water separation and hence not suitable for  
43 the large scale oil water separation (Feng et al., 2004; Zhang et al., 2013). To overcome the

44 clogging and fouling of the oil-water separation filters, materials having superhydrophilic and  
45 underwater superoleophobic properties have been reported (Xue et al., 2011; Ding et al., 2012;  
46 Chen and Xu, 2013; Liu et al., 2013; Xu et al., 2013; Cai et al., 2014; Darmanin and Guittard,  
47 2014; Manna and Lynn, 2015). Various underwater superoleophobic materials such as, titanium  
48 dioxide thin films (Sawai et al., 2013; Zhang et al., 2013; Gondal et al., 2014; Wang and Guo,  
49 2014; Jo and Kim, 2015) polyacrylamide hydrogel coated mesh (Xue et al., 2011), silicates  
50 (Zhang et al., 2013), zinc oxide based mesh (Li et al., 2015), copper oxide covered mesh (Cheng  
51 et al., 2013; Liu et al., 2013), PANI nanowire films (Ding et al., 2012) etc. have been reported.  
52 Fabrication of superhydrophilic and underwater superoleophobic membranes is based on the  
53 coating of nano/micro hierarchical coating of highly polar material on a suitable substrate i.e.  
54 stainless steel (Bellanger et al., 2014; Cai et al., 2014; Darmanin and Guittard, 2014). According  
55 to the extended Young theories, (Young, 1805) it can be expected that underwater  
56 superoleophobic materials could be superhydrophilic in air (Bellanger et al., 2014; Cai et al.,  
57 2014) such that superhydrophilic materials in air should be suitable to prepare underwater  
58 superoleophobic solid surfaces.

59 Titanium dioxide is one of the heavily used inorganic materials in energy and  
60 environmental related applications (Hashimoto et al., 2005; Muneer et al., 2005; Thavasi et al.,  
61 2008). It is a well-known potential semiconductor photocatalyst which can degrade various  
62 organic pollutants with the aid of UV light (Turchi et al., 1990; Tayade et al., 2006; Choi et al.,  
63 2007). In the photocatalytic degradation process, the titanium dioxide surface functions as an  
64 adsorption midpoint to the organic molecules and the adsorbed molecules oxidize to CO<sub>2</sub> and  
65 H<sub>2</sub>O with the aid of hydroxyl radicals (Nagaveni et al., 2004; Choi et al., 2007; Hathway, 2009;  
66 Pan et al., 2012). Hence, when the TiO<sub>2</sub> photocatalyst is fixed in a membrane, TiO<sub>2</sub> coated

67 membrane could have both light induced cleaning property as well as underwater  
68 superoleophobic property (Zhang et al., 2013).

69 For effective oil water separation, a membrane with a highly rough surface is necessary  
70 to achieve stable superhydrophilic property. Highly rough surfaces can be obtained by deposition  
71 of randomly oriented 1-D structures on suitable substrates (Marmur, 2003). Considering the  
72 hydrophilicity,  $\text{TiO}_2$  with 1-D structures such as nanotubes, nanowires or fibrous  $\text{TiO}_2$   
73 structures are suitable materials for the fabrication of underwater superoleophobic filters. In this  
74 study, we fabricated superhydrophilic, nano-structured  $\text{TiO}_2$  nanofibers on stainless steel mesh  
75 by the spray coating technique. The synthesis of  $\text{TiO}_2$  nanofibers is simple and cost effective as  
76 well as  $\text{TiO}_2$  nanofibers exhibit high repellency towards oil in under water. The  
77 micro/nanohierarchical coating of nano-structured  $\text{TiO}_2$  fibers on mesh results in enhanced  
78 surface roughness and underwater superoleophobicity. The oil-water separation method is  
79 basically forward under gravity and shows excellent oil-water separation and the higher oil  
80 contact angle under water with a good recycling efficiency. Finally, the  $\text{TiO}_2$  nanofibers coated  
81 stainless steel meshes possess both underwater superoleophobicity and self-cleaning properties.

## 82 **EXPERIMENTAL SECTION**

### 83 **Preparation of $\text{TiO}_2$ nanofibers and fabrication of $\text{TiO}_2$ nanofibers coated stainless steel** 84 **mesh**

85  $\text{TiO}_2$  nanofibers were prepared by hydrothermal method. To prepare  $\text{TiO}_2$  nanofibers, 2.0  
86 g of  $\text{TiO}_2$  nanoparticles (Degussa P25  $\text{TiO}_2$ ) was stirred with 30 ml of 10 mol/L  $\text{NaOH}_{(\text{aq})}$  (Sigma  
87 Aldrich) solution for 1 h and the suspension was transferred to a 40 ml volume Teflon chamber  
88 until it filled 75% the volume of the chamber and the chamber was fixed into a hydrothermal

89 autoclave vessel. The vessel was allowed to heat at 170°C for 80 h in the furnace and the  
90 hydrothermally synthesized nano sodium-titanate suspension was collected at room temperature.  
91 The pH of the nanofibers was taken down to ~7.5-8.5 by washing with 1 mol/L HCl<sub>(aq)</sub> and  
92 distilled water (Kim et al., 2006) and separated by centrifuging the suspension. These TiO<sub>2</sub>  
93 nanofibers were coated on the stainless steel mesh (#150 micron opening width, size 2''×2''  
94 which were ultrasonically cleaned in acetone and then rinsed with ethanol and deionized water)  
95 by spraying the TiO<sub>2</sub> nanofiber suspension. To prepare TiO<sub>2</sub> nanofibers suspension, 10.0 g of  
96 nanofibers were suspended in 100 ml of 99.9% ethanol solution and sonicated for 10 min and  
97 stirred for 4 h. As prepared TiO<sub>2</sub> nanofibers suspension was sprayed to a pre-cleaned stainless  
98 steel by air brush spraying tool. The TiO<sub>2</sub> nanofibers coated mesh was sintered at 450°C for 45  
99 min and cooled down to room temperature and finally it was rinsed with deionized water to  
100 remove excess or unbound TiO<sub>2</sub> nanofibers.

### 101 **Oil/water separation experiments**

102 The oil/water separation setup was prepared by fixing TiO<sub>2</sub> nanofibers coated stainless  
103 steel mesh into a PVC union setup as shown in Figure S1 in the supporting information. The  
104 water/oil mixture was prepared by mixing 15 g of engine oil (SAE 10W-30) and 40 g of water.  
105 The TiO<sub>2</sub> nanofibers coated mesh was pre-wetted with water before initiating the filtration and  
106 the water/oil mixture (8:3 w/w) was poured to the filtration set up (~ 20 cm<sup>2</sup> area of the mesh  
107 surface coated with ~6.0 mg of TiO<sub>2</sub> nanofibers having surface area of 37 m<sup>2</sup>/g) at the rate of 2.0  
108 ml/s under the gravity. Water was collected into a beaker under the PVC union setup. The TiO<sub>2</sub>  
109 nanofibers coated mesh was rinsed with distilled water to remove the trapped oil droplets from  
110 the mesh after every filtration step. The separation efficiency ( $\vartheta$ ) was calculated by  $\vartheta = (m_{\text{remains}})/(m_{\text{initial}}) \times 100\%$ , where  $m_{\text{remains}}$  and  $m_{\text{initial}}$  are the mass of the oil before and after the  
111

112 separation. The procedure for measurement of the oil mass in the experiment is given in the SI.  
113 The recycle efficiency was obtained by repeating the procedure for 20 cycles and the procedure  
114 was repeated for several oils (silicon oil, 1-octadecane, rapeseed oil and kerosene) to get the  
115 efficiency and stability of the filter for different oils.

#### 116 **Flow-down (membrane) photocatalytic activity**

117 To check the flow through photocatalytic organic purification activity of TiO<sub>2</sub> nanofibers  
118 coated stainless steel mesh, TiO<sub>2</sub> nanofibers coated mesh was fixed between a union and 50 ml  
119 of 20 ppm methylene blue (MB, Aldrich) aqueous solution was subjected to flow at a rate of 1.6  
120 ml/min from a peristaltic pump (Watson Marlow peristaltic pump 120S, 1-32 rpm, 102R single  
121 channel pump head, tube bore 0.8 mm, rate 1.6 ml/min) into the TiO<sub>2</sub> nanofibers coated mesh.  
122 UV light was irradiated on top of the union at 2520 J/m<sup>2</sup> by Atlas Suntest CPS plus UV range  
123 300-800 nm. This procedure was applied to complete 20 cycles. The concentrations of the MB  
124 solutions during the cycles were obtained by measuring the maximum absorbance of the blue  
125 colored solution at 665 nm.

#### 126 **Instrumentation and characterization**

127 Scanning electron microscope (SEM) images was taken by Carl Zeiss EVO LS15  
128 scanning electron microscope, Fourier transform infrared spectroscopy (FTIR) was recorded  
129 from Thermo Nicolet 6700 FTIR machine, UV-Visible spectroscopy data were taken from  
130 Shimadzu 2450 UV-vis spectrophotometer. Contact angle images were taken from the JYSP-360  
131 united test contact angle goniometer. Crystallographic data was taken from Ultima IV X-ray  
132 diffractometer.

133

134 **RESULTS AND DISCUSSION**

135 In this study, we fabricated 1-D TiO<sub>2</sub> nanofibers on stainless steel mesh to achieve  
136 superior superhydrophilicity properties. Nanofibers of TiO<sub>2</sub> were synthesised by hydrothermal  
137 method using TiO<sub>2</sub> powder and NaOH. In the process of formation of nanofibers, the TiO<sub>2</sub>  
138 powder reacted with NaOH to form sheet-like titanate (i.e. layered sodium titanate) and  
139 subsequently these nanosheets were transformed into other structures like nanotube, wires, fibers  
140 etc., by exfoliated from layered sodium titanate. The detail mechanism of formation of different  
141 TiO<sub>2</sub> structures can be found in previous studies (Bavykin et al., 2004; Tsai and Teng, 2004;  
142 Morgan et al., 2008). The SEM image of as synthesised TiO<sub>2</sub> nanofibers is shown in Figure 1a  
143 and the magnified SEM image of TiO<sub>2</sub> nanofibers is shown in Figure S2 of SI. The SEM image  
144 of as synthesized TiO<sub>2</sub> nanofibers reveals that the average length and diameter of the  
145 hydrothermally synthesized titania nanofibers are 20  $\mu\text{m}$  and 150 nm respectively. A detailed  
146 analysis of nanofibers shown in Figure S2 indicates individually grown nanofibers are not  
147 connected to each other. Interestingly most nanofibers exhibit rigid structure. These TiO<sub>2</sub>  
148 nanofibers were coated on the stainless steel. The uncoated stainless steel mesh surface and TiO<sub>2</sub>  
149 nanofibers coated stainless steel meshes are illustrated in Figure 1b and 1c respectively. As  
150 shown in Figure 1c, the smooth stainless steel surface is completely covered with randomly  
151 oriented TiO<sub>2</sub> nanofibers resulting in a highly rough surface. The thickness of the coated TiO<sub>2</sub>  
152 nanofibers on stainless mesh can be estimated as follows; the pore diameter of bare mesh which  
153 is 150  $\mu\text{m}$  (Figure 1b) has been reduced to  $\sim 130$   $\mu\text{m}$  after coating of TiO<sub>2</sub> nanofibers (Figure 1c)  
154 on the mesh and hence it can be deduced a  $\sim 10$   $\mu\text{m}$  thick TiO<sub>2</sub> layer on the surface of the mesh.  
155 The magnified SEM image of TiO<sub>2</sub> nanofibers coated mesh (Figure 1d) indicates that the TiO<sub>2</sub>  
156 nanofibers coated stainless steel mesh has both micro and nanoscale surface roughness which is

157 more important for manipulating the advance surface wettability. This type of micro/nano  
158 surface structure of the modified stainless steel mesh is more favorable to attract water and repel  
159 oil underwater which exhibits underwater superoleophobicity as a result of high surface  
160 roughness properties of these micro/nano surface structures (Wang et al., 2015).

161 It is known that the surface wetting behavior depends on chemical composition of the  
162 surface. Hence, in addition to the micro/nano morphological structure of the material, the wetting  
163 properties of a surface also highly depend on the chemical composition of the surface (Shin et  
164 al., 2016). Therefore, surface bonding properties of upper exposed layer of TiO<sub>2</sub> nanofibers were  
165 characterized by the FTIR analysis and shown in Figure 2. The broad band at the 3450 cm<sup>-1</sup> and  
166 a weak band at 1658 cm<sup>-1</sup> can be attributed to O-H vibrational stretching mode and the  
167 vibrational bending mode with the adsorbed water molecules respectively. These peaks reveal  
168 that the hydrothermally modified titanate surface has outer layered and interlayered O-H groups  
169 (Ferreira et al., 2006). Specially the broadening effect at the band near 3500 cm<sup>-1</sup> indicate the  
170 formation of different O-H groups on the Ti-OH surface due to adsorption of water molecules  
171 on hydrothermally synthesized TiO<sub>2</sub> nanofibers (Xu et al., 2014). The dominant intense band at  
172 457 cm<sup>-1</sup> and 730 cm<sup>-1</sup> could be attributed to different types of Ti-O-Ti vibrations (Nikolić et al.,  
173 2008) and the peak at 920 cm<sup>-1</sup> indicates the Ti-O non bridging oxygen bonds and it may assign  
174 to Ti-O-Na bond types in the titanate structure (Nikolić et al., 2008). Such chemical composition  
175 and the bond polarity favor attraction of water easily on the surface of TiO<sub>2</sub> nanofibers coated  
176 mesh permitting it to acts as superhydrophilic membrane.

177 The X-ray diffraction patterns of TiO<sub>2</sub> nanofibers calcined at 450 °C were investigated  
178 and the results are given in the supporting information in Figure S3. XRD analyses indicate the  
179 existence of three possible crystals structures (anatase TiO<sub>2</sub>, Ti<sub>5</sub>O<sub>9</sub> and Na<sub>2</sub>Ti<sub>20</sub>O<sub>25</sub>) in the

180 synthesized nanofibers and details of crystalline structures are given in SI. The binding property  
181 of TiO<sub>2</sub> nanofibers on to the mesh is an important parameter when fabricating filters. However, a  
182 clear bonding mechanism between TiO<sub>2</sub> and stainless steel mesh is unknown, but it has been  
183 proposed a diffuse bonding (it is a combination of mechanical compaction and chemical  
184 formation) between TiO<sub>2</sub> and steel mesh (Kliemann et al., 2011). Interestingly, adhesion test  
185 (see Figure S4) confirms that TiO<sub>2</sub> nanofibers are firmly bound to mesh and only loosely bound  
186 TiO<sub>2</sub> nanofibers are detached from the surface.

187

### 188 **Wetting performance and underwater contact angle of the TiO<sub>2</sub> nanofibers coated** 189 **membranes**

190 For efficient oil-water separation, the wettability of the filter plays a big role and it is an  
191 important parameter. Despite the TiO<sub>2</sub> nanofibers coated mesh exhibits superhydrophilicity as  
192 well as oleophilicity in air, wetting rates of water and oil on the TiO<sub>2</sub> nanofibers coated mesh are  
193 different. i.e. water droplets spread completely on the TiO<sub>2</sub> nanofibers coated mesh instantly  
194 (with a static contact angle of  $\sim 0^\circ$ ) while complete spreading of an oil droplet on the TiO<sub>2</sub>  
195 nanofibers coated mesh takes  $\sim 10$  s in air. As shown in Figure 3a, the bare stainless steel mesh  
196 exhibits the water contact angle of  $\sim 96^\circ$  in air and at the same time it exhibits underwater  
197 oleophilicity with a contact angle of  $\sim 68^\circ$  (Figure 3d). As explained earlier and shown in Figure  
198 3b and 3c, TiO<sub>2</sub> nanofibers coated mesh shows superhydrophilic as well as oleophilic natures  
199 respectively in air. Interestingly, the TiO<sub>2</sub> nanofibers coated mesh shows underwater oleophobic  
200 property as shown in Figure 3e. The underwater contact angle of 1,2- dichloroethane with TiO<sub>2</sub>  
201 nanofibers coated membrane is shown in the Figure 3f. As shown in Figure 3f, an underwater oil

202 contact angle of  $162^\circ$  confirms the superoleophobic property of the  $\text{TiO}_2$  nanofibers coated mesh  
203 in underwater condition.

204 The Young's equation can be used to explain the contact angel of solid-air, solid-water,  
205 water-air, solid-oil, oil-air interfaces and this equation can be extended to an underwater oil  
206 droplets in solid surfaces as oil/water/solid systems (Cai et al., 2014). According to extended  
207 Young's equation, it can be expected that underwater superoleophobic materials could be  
208 hydrophilic in air. From contact angel measurements, it is clearly demonstrated the  
209 superoleophobic properties of the  $\text{TiO}_2$  nanofibers coated mesh in underwater condition  
210 compared to bare mesh. As such, an efficient separation of oil and water with  $\text{TiO}_2$  nanofibers  
211 coated mesh can be expected. In a very recent publication, Jo and Kim et al, reported oil water  
212 separation using  $\text{TiO}_2$  nanopartciles on mesh (Jo and Kim, 2015). Yet our system is different as  
213 we have used  $\text{TiO}_2$  nanofibers with nano/micro hierarchical behavior where a higher Cassie-  
214 Baxter state can be expected with  $\text{TiO}_2$  nanofibers and hence enhanced liquid repelling material  
215 surface underwater. Especially here we have discussed the dual properties of underwater  
216 superoleophobicity and self-cleaning and photocatalytic activity of the membrane.

217 As described earlier, the  $\text{TiO}_2$  nanofibers coated mesh has a great potential to repel oil  
218 under water due to superoleophobic properties in under water. In this study, water-oil separation  
219 efficiency was used to investigate the  $\text{TiO}_2$  nanofibers modified mesh as an oil-water separation  
220 filter. The simple water/oil separation setup is illustrated in Figure 4a where the bare mesh (left)  
221 or  $\text{TiO}_2$  nanofibers coated filter mesh (right) is fixed in a commercially available PVC union  
222 joint. Mixture of commercial engine oil (SAE 10W-30): water in 3:8 (w/w) ratio was passed  
223 through the pre-wetted filter under the gravity without any extra force. In this experiment, water  
224 is blue colored for clarity and the color of the oil is brown. As shown in Figure 4a, both water

225 and oil permeated through the bare mesh, while with the TiO<sub>2</sub> coated mesh, separation of engine  
226 oil (yellow-brown color) and the water (blue color) is clearly visible.

227 Different types of oil/water mixtures were passed through the TiO<sub>2</sub> coated mesh to check the  
228 feasibility of the separation including silicon oil, rapeseed oil, kerosene, 1-octadecene and engine  
229 oil and the individual separation efficiency of different oils can be seen in Figure 4b after one  
230 separation cycle. As shown in Figure 4b, separation efficiencies of ~99 and ~90% can be  
231 achieved with high viscous oil (silicon oil) and low viscous oil (kerosene) respectively. The filter  
232 made with TiO<sub>2</sub> nanofibers on the stainless steel mesh was tested for its durability by using the  
233 same filter for several separation cycles of oil-water mixture and the oil water separation  
234 efficiency with the separation cycles are shown in Figure 4c. From the Oil water separation  
235 results shown in Figure 4c, it is clear that at each separation cycle, over 97.5 ( $\pm 1.8$ )% separation  
236 efficiency was achieved where water in the mixture passed through the mesh quickly, and no  
237 visible oil was observed in the collected water.

### 238 **Photocatalytic activity and self-cleaning property of the membrane**

239 The TiO<sub>2</sub> nanofibers coated stainless steel mesh can function as a heterogeneous catalyst  
240 to degrade toxic organic matters at the same time with the oil water separation and hence it has  
241 the underwater self-cleaning property. To verify the photocatalytic property, MB solution was  
242 allowed to flow through the membrane under the gravity while the system was subjected to UV  
243 irradiation as shown in Figure 5a. The MB solution was passed through the mesh for few cycles  
244 to touch the MB solution on the semiconductor TiO<sub>2</sub> nanofibers to degrade the organic molecules  
245 more efficiently. The disappearance (or the degradation) of MB after passing through the  
246 membrane in the presence of UV light is clearly visible as shown in the image (right side) of  
247 Figure 5a. The degradation of MB with the reaction time was monitored by the UV visible

248 spectra and shown in Figure 5b. As shown in Figure 5b, the concentration of the MB solution  
249 was reduced from 20.0 ppm to 2.6 ppm within 20 cycles. The reduction of MB concentration  
250 could be due to both adsorption and degradation. The flow through process in the dark confirms  
251 that the concentration of the MB solution has dropped 20.0 ppm to 15.0 ppm within 20 cycles  
252 due to adsorption of MB on the surface of TiO<sub>2</sub> nanofibers. As well, a significant concentration  
253 drop (from 20 ppm to 0.6 ppm) is observed when the mesh allowed to retain in the 20.0 ppm  
254 static MB solution under UV light. In the degradation process of MB on TiO<sub>2</sub> photocatalyst, an  
255 electron can be promoted to the conduction band from the valence band at the photoexcitation  
256 which exceeding the energy of the band gap (3.23 eV), (Butler and Ginley, 1980; Nogueira and  
257 Jardim, 1993; Zhao et al., 1998) producing an e-h pair. The excited electron would react with  
258 adsorbed oxygen or reduce the adsorbed MB on TiO<sub>2</sub>. While, the photo induced hole can react  
259 with adsorbed MB or form hydroxyl radical which is also a strong oxidative species. (Houas et  
260 al., 2001) The organic pollutant MB can be oxidized to CO<sub>2</sub>, SO<sub>4</sub><sup>2-</sup>, NH<sub>4</sub><sup>+</sup> and NO<sub>3</sub><sup>-</sup> through  
261 several steps by hydroxyl radicals or holes. (Nogueira and Jardim, 1993)



263  
264 Figure 5b indicates the degradation of the MB organic solution through the discoloration of the  
265 blue color. The degradation efficiency is highly depends on the MB adsorption rate on TiO<sub>2</sub>  
266 fibers, active area of the mesh and the intensity of the UV light. This underwater  
267 superoleophobic mesh can efficiently remove not only the immiscible oil but also organic  
268 contaminants in the water.

269

**270 CONCLUSION**

271 Superhydrophilic and underwater superoleophobic behavior of the hydrothermally synthesized  
272 TiO<sub>2</sub> nanofibers coated stainless steel mesh is investigated. The TiO<sub>2</sub> nanofibers coated stainless  
273 steel mesh shows the water contact angle of 0°-2° and the oil contact angle of 162° at the air and  
274 under water respectively to prove the superhydrophilic and underwater superoleophobic  
275 nature. The membrane can successfully separate different types of oil from water with a  
276 separation efficiency of over ~99% and the photocatalytic effect of the membrane helps to  
277 separate not only the immiscible oil but also the miscible organics from the water.

278

**279 ACKNOWLEDGMENT**

280 This work was financially supported by under the grant of RG/2012/ESA/01, National Science  
281 Foundation, Sri Lanka. Special thanks to Rushdi Senevirathne, Shanka Dissanayake and Dulanji  
282 Dharmagunawardhane for the technical assistant for sample characterization

## 283 REFERENCES

- 284 Al-Shamrani, A., James, A., Xiao, H., 2002. Destabilisation of oil–water emulsions and  
285 separation by dissolved air flotation. *Water Research* 36, 1503-1512.
- 286 Balba, M., Al-Awadhi, N., Al-Daher, R., 1998. Bioremediation of oil-contaminated soil:  
287 microbiological methods for feasibility assessment and field evaluation. *Journal of*  
288 *microbiological methods* 32, 155-164.
- 289 Bautista, P., Mohedano, A., Casas, J., Zazo, J., Rodriguez, J., 2008. An overview of the  
290 application of Fenton oxidation to industrial wastewaters treatment. *J. Chem. Tech. Biotech.* 83,  
291 1323-1338.
- 292 Bavykin, D.V., Parmon, V.N., Lapkin, A.A., Walsh, F.C., 2004. The effect of hydrothermal  
293 conditions on the mesoporous structure of TiO<sub>2</sub> nanotubes. *J. Mater. Chem.* 14, 3370-3377.
- 294 Bellanger, H., Darmanin, T., Taffin de Givenchy, E., Guittard, F., 2014. Chemical and physical  
295 pathways for the preparation of superoleophobic surfaces and related wetting theories. *Chemical*  
296 *reviews* 114, 2694-2716.
- 297 Bratby, J., 1980. *Coagulation and flocculation*. England: Uplands.
- 298 Butler, M., Ginley, D., 1980. Principles of photoelectrochemical, solar energy conversion. *J.*  
299 *Mater. Sci.* 15, 1-19.
- 300 Cai, Y., Lin, L., Xue, Z., Liu, M., Wang, S., Jiang, L., 2014. Filefish-Inspired Surface Design for  
301 Anisotropic Underwater Oleophobicity. *Advanced Functional Materials* 24, 809-816.
- 302 Chen, P.-C., Xu, Z.-K., 2013. Mineral-coated polymer membranes with superhydrophilicity and  
303 underwater superoleophobicity for effective oil/water separation. *Scientific reports* 3.
- 304 Cheng, Z., Lai, H., Du, Y., Fu, K., Hou, R., Zhang, N., Sun, K., 2013. Underwater  
305 Superoleophilic to Superoleophobic Wetting Control on the Nanostructured Copper Substrates.  
306 *ACS Applied Materials & Interfaces* 5, 11363-11370.
- 307 Choi, H., Stathatos, E., Dionysiou, D.D., 2007. Photocatalytic TiO<sub>2</sub> films and membranes for the  
308 development of efficient wastewater treatment and reuse systems. *Desalination* 202, 199-206.
- 309 Chong, M.N., Jin, B., Chow, C.W., Saint, C., 2010. Recent developments in photocatalytic water  
310 treatment technology: a review. *Water research* 44, 2997-3027.
- 311 Darmanin, T., Guittard, F., 2014. Wettability of conducting polymers: From superhydrophilicity  
312 to superoleophobicity. *Progress in Polymer Science* 39, 656-682.
- 313 Ding, C., Zhu, Y., Liu, M., Feng, L., Wan, M., Jiang, L., 2012. PANI nanowire film with  
314 underwater superoleophobicity and potential-modulated tunable adhesion for no loss oil droplet  
315 transport. *Soft Matter* 8, 9064-9068.
- 316 Dunderdale, G.J., Urata, C., Sato, T., England, M.W., Hozumi, A., 2015. Continuous, High-  
317 Speed, and Efficient Oil/Water Separation using Meshes with Antagonistic Wetting Properties.  
318 *ACS Applied Materials & Interfaces* 7, 18915-18919.
- 319 Fakhru'l-Razi, A., Pendashteh, A., Abdullah, L.C., Biak, D.R.A., Madaeni, S.S., Abidin, Z.Z.,  
320 2009. Review of technologies for oil and gas produced water treatment. *Journal of Hazardous*  
321 *Materials* 170, 530-551.
- 322 Feng, L., Zhang, Z., Mai, Z., Ma, Y., Liu, B., Jiang, L., Zhu, D., 2004. A super-hydrophobic and  
323 super-oleophilic coating mesh film for the separation of oil and water. *Angew. Chem. Int. Ed.*  
324 43, 2012-2014.
- 325 Ferreira, O.P., Souza Filho, A.G., Mendes Filho, J., Alves, O.L., 2006. Unveiling the structure  
326 and composition of titanium oxide nanotubes through ion exchange chemical reactions and  
327 thermal decomposition processes. *Journal of the Brazilian Chemical Society* 17, 393-402.

- 328 Fosberg, T., 1974. Method and apparatus for detecting oil pollution in water. Google Patents.  
329 Gaya, U.I., Abdullah, A.H., 2008. Heterogeneous photocatalytic degradation of organic  
330 contaminants over titanium dioxide: a review of fundamentals, progress and problems. *Journal of*  
331 *Photochemistry and Photobiology C: Photochemistry Reviews* 9, 1-12.
- 332 Gondal, M.A., Sadullah, M.S., Dastageer, M.A., McKinley, G.H., Panchanathan, D., Varanasi,  
333 K.K., 2014. Study of Factors Governing Oil–Water Separation Process Using TiO<sub>2</sub> Films  
334 Prepared by Spray Deposition of Nanoparticle Dispersions. *ACS Applied Materials & Interfaces*  
335 6, 13422-13429.
- 336 Gur-Reznik, S., Katz, I., Dosoretz, C.G., 2008. Removal of dissolved organic matter by granular-  
337 activated carbon adsorption as a pretreatment to reverse osmosis of membrane bioreactor  
338 effluents. *Water research* 42, 1595-1605.
- 339 Hashimoto, K., Irie, H., Fujishima, A., 2005. TiO<sub>2</sub> photocatalysis: a historical overview and  
340 future prospects. *Japanese journal of applied physics* 44, 8269.
- 341 Hathway, T.L., 2009. Titanium dioxide photocatalysis: studies of the degradation of organic  
342 molecules and characterization of photocatalysts using mechanistic organic chemistry.
- 343 Houas, A., Lachheb, H., Ksibi, M., Elaloui, E., Guillard, C., Herrmann, J.-M., 2001.  
344 Photocatalytic degradation pathway of methylene blue in water. *Applied Catalysis B:*  
345 *Environmental* 31, 145-157.
- 346 Inan, H., Dimoglo, A., Şimşek, H., Karpuzcu, M., 2004. Olive oil mill wastewater treatment by  
347 means of electro-coagulation. *Separation and purification technology* 36, 23-31.
- 348 Jo, S., Kim, Y., 2015. Superhydrophilic–underwater superoleophobic TiO<sub>2</sub>-coated mesh for  
349 separation of oil from oily seawater/wastewater. *Korean J. Chem. Eng.*, 1-4.
- 350 Kim, G.-S., Seo, H.-K., Godble, V., Kim, Y.-S., Yang, O.-B., Shin, H.-S., 2006. Electrophoretic  
351 deposition of titanate nanotubes from commercial titania nanoparticles: application to dye-  
352 sensitized solar cells. *Electrochemistry Communications* 8, 961-966.
- 353 Kliemann, J.-O., Gutzmann, H., Gärtner, F., Hübner, H., Borchers, C., Klassen, T., 2011.  
354 Formation of cold-sprayed ceramic titanium dioxide layers on metal surfaces. *J. Therm. Spray*  
355 *Technol.* 20, 292-298.
- 356 Lee, C.H., Johnson, N., Drelich, J., Yap, Y.K., 2011. The performance of superhydrophobic and  
357 superoleophilic carbon nanotube meshes in water–oil filtration. *Carbon* 49, 669-676.
- 358 Li, J., Yan, L., Li, W., Li, J., Zha, F., Lei, Z., 2015. Superhydrophilic–underwater  
359 superoleophobic ZnO-based coated mesh for highly efficient oil and water separation. *Mater.*  
360 *Lett.* 153, 62-65.
- 361 Liu, J., Diamond, J., 2005. China's environment in a globalizing world. *Nature* 435, 1179-1186.
- 362 Liu, N., Chen, Y., Lu, F., Cao, Y., Xue, Z., Li, K., Feng, L., Wei, Y., 2013. Straightforward  
363 oxidation of a copper substrate produces an underwater superoleophobic mesh for oil/water  
364 separation. *ChemPhysChem* 14, 3489-3494.
- 365 Ma, H., Wang, B., 2006. Electrochemical pilot-scale plant for oil field produced wastewater by  
366 M/C/Fe electrodes for injection. *Journal of hazardous materials* 132, 237-243.
- 367 Manna, U., Lynn, D.M., 2015. Synthetic Surfaces with Robust and Tunable Underwater  
368 Superoleophobicity. *Advanced Functional Materials*.
- 369 Marmur, A., 2003. Wetting on hydrophobic rough surfaces: to be heterogeneous or not to be?  
370 *Langmuir* 19, 8343-8348.
- 371 Mitchell, B.G., Kahru, M., Wieland, J., Stramska, M., 2002. Determination of spectral absorption  
372 coefficients of particles, dissolved material and phytoplankton for discrete water samples. *Ocean*  
373 *optics protocols for satellite ocean color sensor validation, Revision 3*, 231-257.

- 374 Morgan, D.L., Zhu, H.-Y., Frost, R.L., Waclawik, E.R., 2008. Determination of a Morphological  
375 Phase Diagram of Titania/Titanate Nanostructures from Alkaline Hydrothermal Treatment of  
376 Degussa P25. *Chem. Mater.* 20, 3800-3802.
- 377 Muneer, M., Qamar, M., Saquib, M., Bahnemann, D., 2005. Heterogeneous photocatalysed  
378 reaction of three selected pesticide derivatives, propham, propachlor and tebuthiuron in aqueous  
379 suspensions of titanium dioxide. *Chemosphere* 61, 457-468.
- 380 Munter, R., 2001. Advanced oxidation processes—current status and prospects. *Proc. Estonian*  
381 *Acad. Sci. Chem* 50, 59-80.
- 382 Nagaveni, K., Sivalingam, G., Hegde, M., Madras, G., 2004. Photocatalytic degradation of  
383 organic compounds over combustion-synthesized nano-TiO<sub>2</sub>. *Environmental science &*  
384 *technology* 38, 1600-1604.
- 385 Nikolić, L.M., Maletin, M., Ferreira, P., Vilarinho, P.M., 2008. Synthesis and characterization of  
386 one-dimensional titanate structure. *Processing and application of ceramics* 2, 109-114.
- 387 Nogueira, R.F., Jardim, W.F., 1993. Photodegradation of methylene blue: Using solar light and  
388 semiconductor (TiO<sub>2</sub>). *J. Chem. Educ.* 70, 861.
- 389 Odeigah, P., Nurudeen, O., Amund, O.O., 1997. Genotoxicity of oil field wastewater in Nigeria.  
390 *Hereditas* 126, 161-167.
- 391 Olsson, G., 2015. Water and energy: threats and opportunities. *Water Intelligence Online* 14,  
392 9781780406947.
- 393 Pan, G., Wang, D., Liu, Y., 2012. Photocatalytic degradation pathways and adsorption modes of  
394 H-acid in TiO<sub>2</sub> suspensions. *Chin. Sci. Bull.* 57, 1102-1108.
- 395 Pyrzynska, K., 2011. Carbon nanotubes as sorbents in the analysis of pesticides. *Chemosphere*  
396 83, 1407-1413.
- 397 Rosal, R., Rodríguez, A., Perdigón-Melón, J.A., Petre, A., García-Calvo, E., Gómez, M.J.,  
398 Agüera, A., Fernández-Alba, A.R., 2010. Occurrence of emerging pollutants in urban wastewater  
399 and their removal through biological treatment followed by ozonation. *Water Research* 44, 578-  
400 588.
- 401 Sawai, Y., Nishimoto, S., Kameshima, Y., Fujii, E., Miyake, M., 2013. Photoinduced underwater  
402 superoleophobicity of TiO<sub>2</sub> thin films. *Langmuir* 29, 6784-6789.
- 403 Schrank, S., José, H., Moreira, R., Schröder, H.F., 2004. Elucidation of the behavior of tannery  
404 wastewater under advanced oxidation conditions. *Chemosphere* 56, 411-423.
- 405 Tayade, R.J., Kulkarni, R.G., Jasra, R.V., 2006. Transition metal ion impregnated mesoporous  
406 TiO<sub>2</sub> for photocatalytic degradation of organic contaminants in water. *Industrial & engineering*  
407 *chemistry research* 45, 5231-5238.
- 408 Thavasi, V., Singh, G., Ramakrishna, S., 2008. Electrospun nanofibers in energy and  
409 environmental applications. *Energy & Environmental Science* 1, 205-221.
- 410 Tsai, C.-C., Teng, H., 2004. Regulation of the physical characteristics of titania nanotube  
411 aggregates synthesized from hydrothermal treatment. *Chem. Mater.* 16, 4352-4358.
- 412 Turchi, C.S., Ollis, D.F., 1990. Photocatalytic degradation of organic water contaminants:  
413 mechanisms involving hydroxyl radical attack. *Journal of catalysis* 122, 178-192.
- 414 Wang, H., Guo, Z., 2014. Design of underwater superoleophobic TiO<sub>2</sub> coatings with additional  
415 photo-induced self-cleaning properties by one-step route bio-inspired from fish scales. *Appl.*  
416 *Phys. Lett.* 104, 183703.
- 417 Wang, J., Do-Quang, M., Cannon, J.J., Yue, F., Suzuki, Y., Amberg, G., Shiomi, J., 2015.  
418 Surface structure determines dynamic wetting. *Scientific reports* 5.

- 419 Wang, S., Song, Y., Jiang, L., 2006. Microscale and nanoscale hierarchical structured mesh films  
420 with superhydrophobic and superoleophilic properties induced by long-chain fatty acids.  
421 *Nanotechnology* 18, 015103.
- 422 Xia, S., Duan, L., Song, Y., Li, J., Piceno, Y.M., Andersen, G.L., Alvarez-Cohen, L., Moreno-  
423 Andrade, I., Huang, C.-L., Hermanowicz, S.W., 2010. Bacterial community structure in  
424 geographically distributed biological wastewater treatment reactors. *Environmental science &*  
425 *technology* 44, 7391-7396.
- 426 Xu, J., Zhang, H., Liu, T., Zhang, J., 2014. Fabrication and Characterization of Potassium and  
427 Sodium Titanate via a Hydrothermal Method. *J. Chem. Soc. Pak* 36, 388.
- 428 Xu, L.-P., Peng, J., Liu, Y., Wen, Y., Zhang, X., Jiang, L., Wang, S., 2013. Nacre-inspired  
429 design of mechanical stable coating with underwater superoleophobicity. *ACS nano* 7, 5077-  
430 5083.
- 431 Xu, P., Zeng, G.M., Huang, D.L., Feng, C.L., Hu, S., Zhao, M.H., Lai, C., Wei, Z., Huang, C.,  
432 Xie, G.X., 2012. Use of iron oxide nanomaterials in wastewater treatment: a review. *Science of*  
433 *the Total Environment* 424, 1-10.
- 434 Xu, Z., Zhao, Y., Wang, H., Zhou, H., Qin, C., Wang, X., Lin, T., 2016. Fluorine-Free  
435 Superhydrophobic Coatings with pH-induced Wettability Transition for Controllable Oil–Water  
436 Separation. *ACS Applied Materials & Interfaces* 8, 5661-5667.
- 437 Xue, Z., Cao, Y., Liu, N., Feng, L., Jiang, L., 2014. Special wettable materials for oil/water  
438 separation. *J. Mater. Chem. A* 2, 2445-2460.
- 439 Xue, Z., Wang, S., Lin, L., Chen, L., Liu, M., Feng, L., Jiang, L., 2011. A Novel  
440 Superhydrophilic and Underwater Superoleophobic Hydrogel-Coated Mesh for Oil/Water  
441 Separation. *Advanced Materials* 23, 4270-4273.
- 442 Yao, X., Song, Y., Jiang, L., 2011. Applications of Bio-Inspired Special Wettable Surfaces.  
443 *Advanced Materials* 23, 719-734.
- 444 Young, T., 1805. An essay on the cohesion of fluids. *Philosophical Transactions of the Royal*  
445 *Society of London*, 65-87.
- 446 Zhang, L., Zhong, Y., Cha, D., Wang, P., 2013. A self-cleaning underwater superoleophobic  
447 mesh for oil-water separation. *Scientific reports* 3.
- 448 Zhao, G., Utsumi, S., Kozuka, H., Yoko, T., 1998. Photoelectrochemical properties of sol–gel-  
449 derived anatase and rutile TiO<sub>2</sub> films. *J. Mater. Sci.* 33, 3655-3659.

450

451

452

453

454

455

456

457

Table 01: Static contact angles of liquids in the medium of water and air

Medium	SS mesh water contact angle	TiO <sub>2</sub> nanofibers coated membrane water contact angle	SS mesh oil contact angle	TiO <sub>2</sub> nanofibers coated membrane oil contact angle
air	96°	0°	0°	0°
Underwater	-	0°	68°	162°

458

459

460

461

462

463

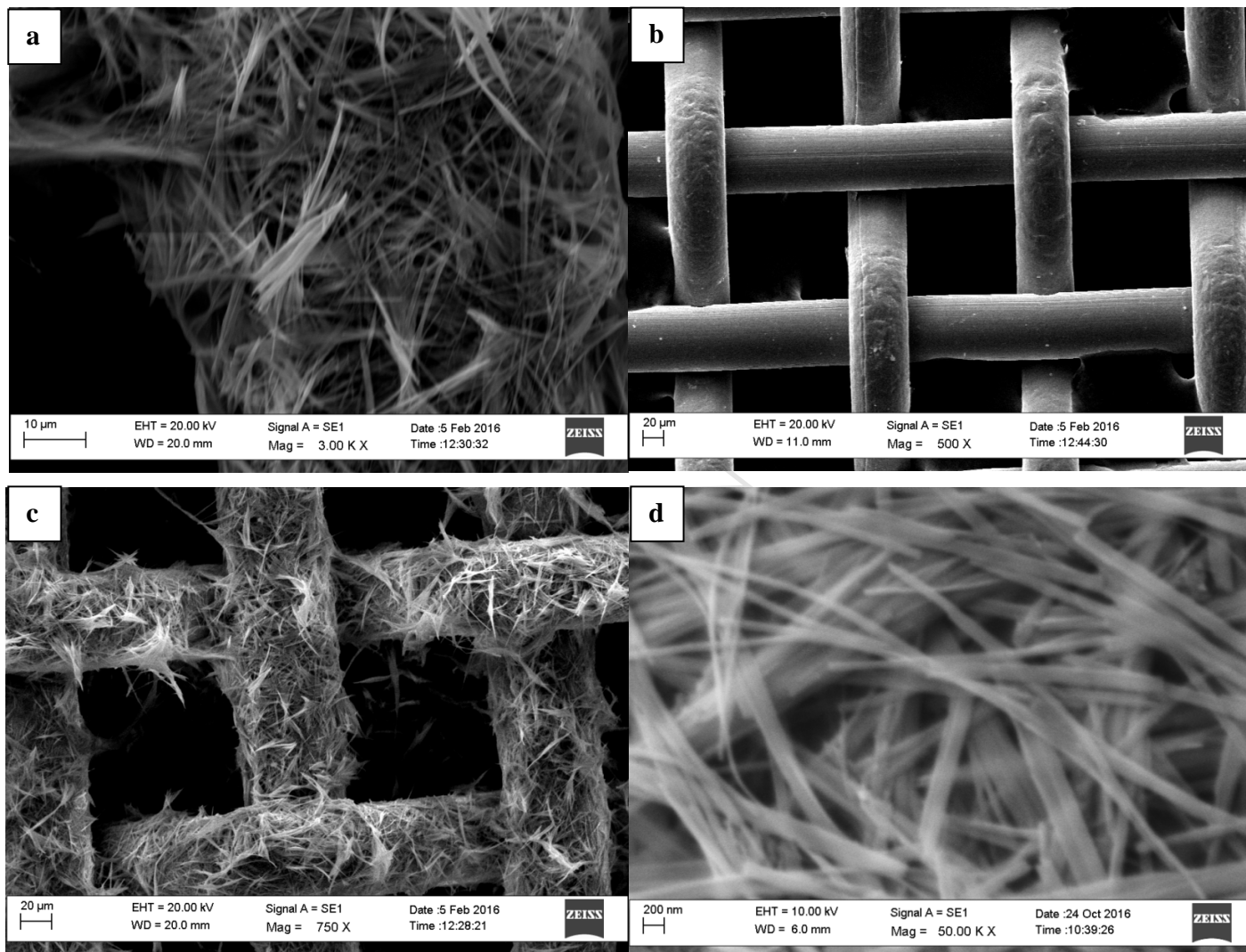
464

465

466

467

468



469

470

471

472

473

474

475

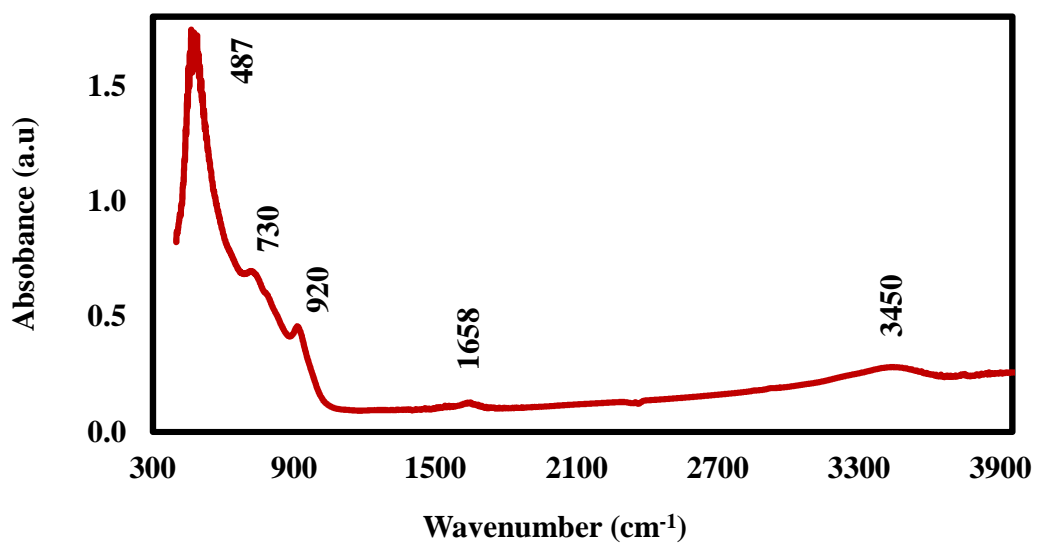
Figure 1

476

477

478

479



480

Figure 2

481

482

483

484

485

486

487

488

489

490

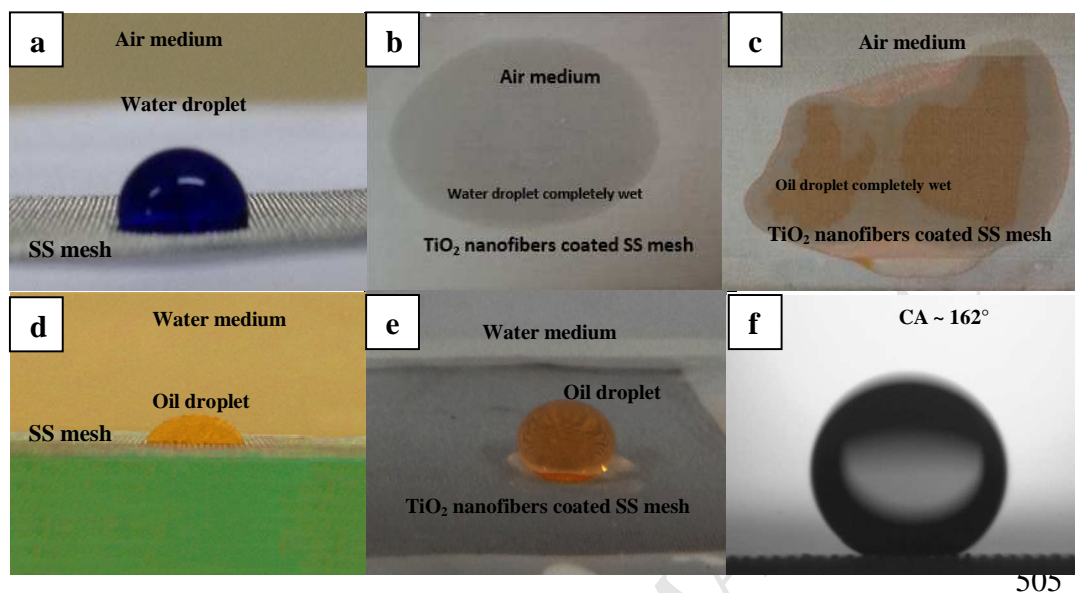
491

492

493

494

495



505

506

507

508

509

510

511

512

513

514

515

516

517

Figure 3

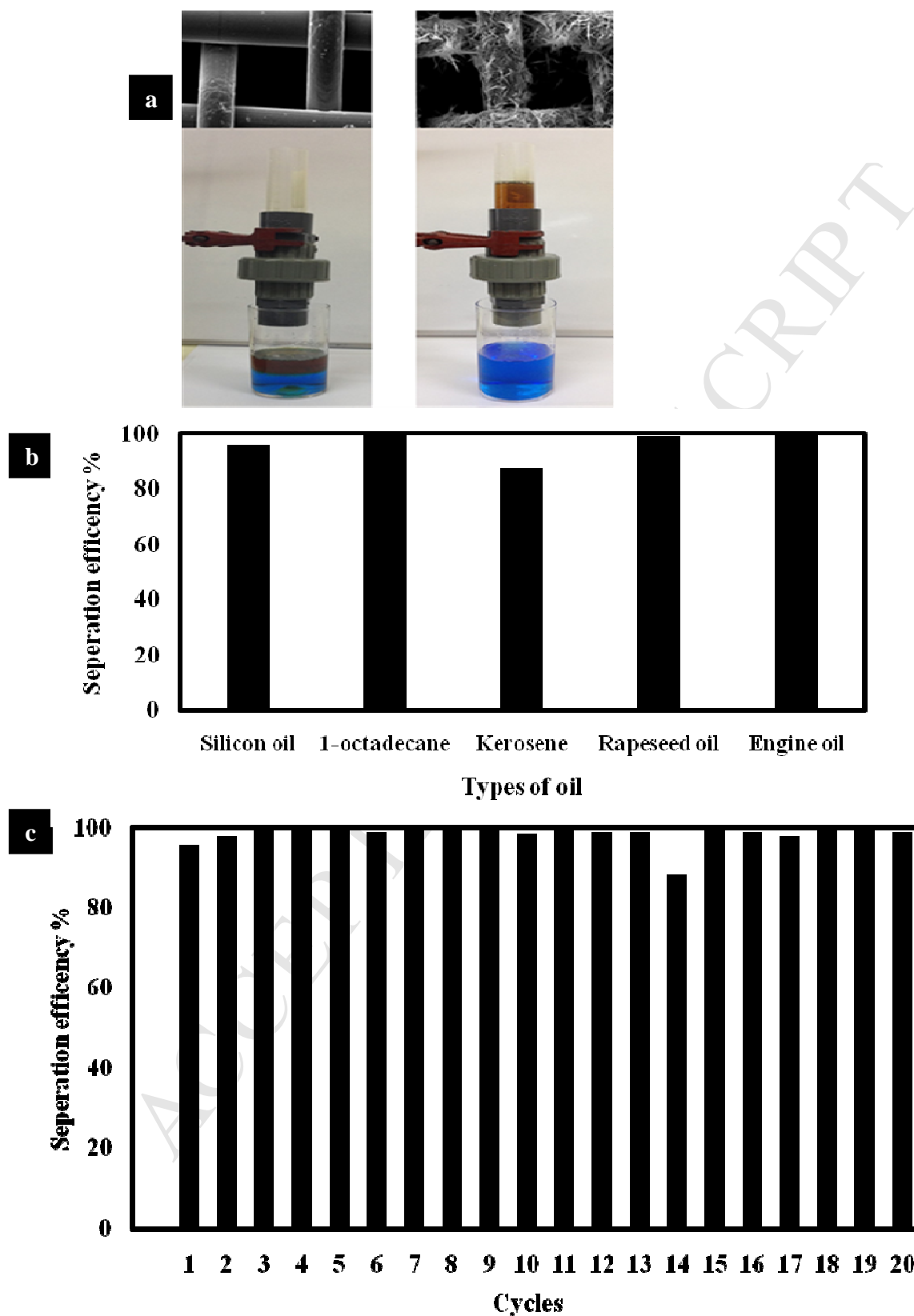
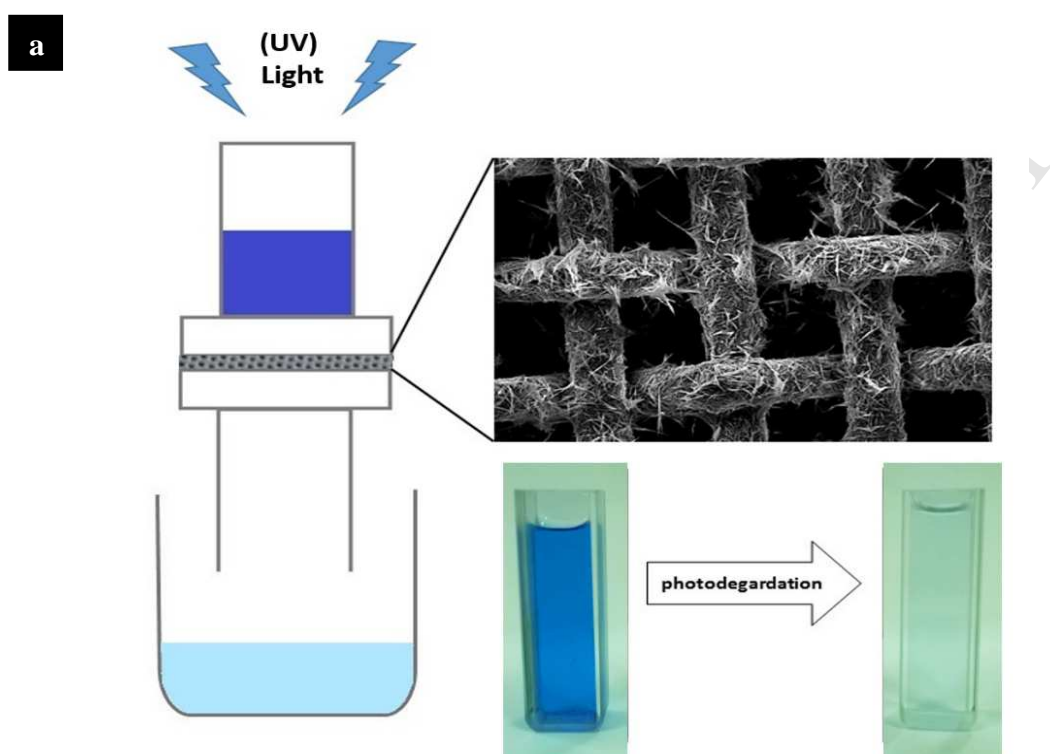
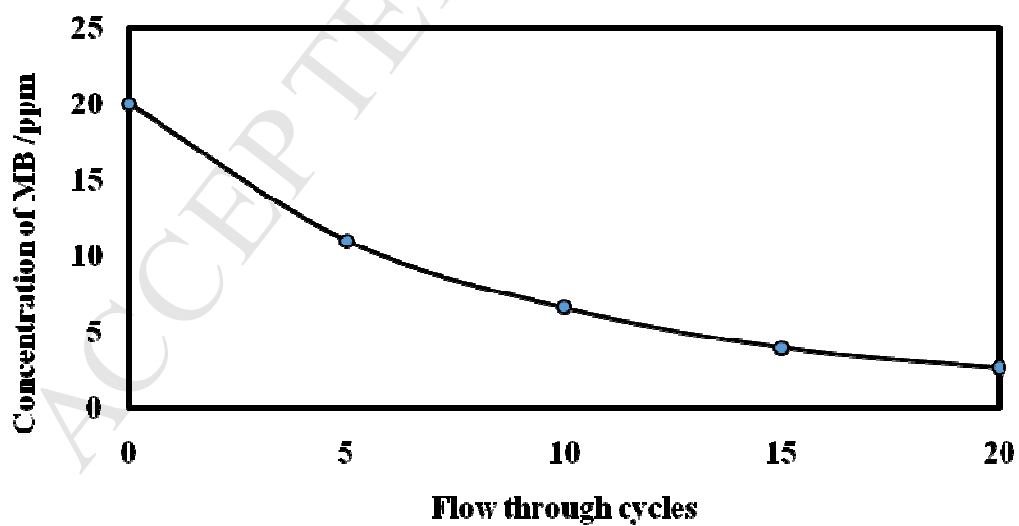
518  
519

Figure 4

520

**b**

521

522

Figure 5

## Figure captions

**Figure 1.** SEM images of (a) TiO<sub>2</sub> nanofibers; (b) original bare stainless steel mesh; (c) low magnification scanning of TiO<sub>2</sub> nanofibers coated stainless steel mesh; (d) high magnification image of TiO<sub>2</sub> nanofibers

**Figure 2.** FTIR spectrum of TiO<sub>2</sub> nanofibers sintered at 450 °C

**Figure 3.** Air medium wetting properties of (a) water droplet on bare stainless steel mesh; (b) water droplet wetted TiO<sub>2</sub> nanofibers coated stainless steel mesh; (c) oil droplet wetted TiO<sub>2</sub> nanofibers coated stainless steel mesh. Underwater wetting properties of oil droplets on (d) bare stainless steel mesh; (e) TiO<sub>2</sub> nanofibers coated stainless steel mesh; (f) contact angle image of oil droplet on TiO<sub>2</sub> nanofibers coated stainless steel mesh underwater obtained by Goniometer.

**Figure 4.** (a) water-oil separation setup of uncoated (left side) and TiO<sub>2</sub> nanofibers coated mesh (right hand side) and separated oil-water from respective filters; (b) separation efficiencies of different oil types; (c) recyclable ability of the TiO<sub>2</sub> nanofibers coated membrane.

**Figure 5.** (a) Flow-down (membrane) photocatalytic activity set up where filter is fixed in the middle of PVC union and irradiated with Suntest CPS light source. The inset shows the color change of MB after irradiation; (b) Change of concentration of methylene blue (MB) with recycle time.

### Highlights

- Highly rough TiO<sub>2</sub> fibers on stainless steel filter was fabricated
- The membrane is Superhydrophilic (underwater superoleophobic).
- The membrane can separate range of oil-water mixtures with the separation efficiency of ~98-99%.
- The modified mesh can degrade immiscible organic molecules due to the photocatalytic activity of TiO<sub>2</sub> nanofibers